Simulations of quantum crystals by classical dynamics

M. Sterling, Z. Li, and V. A. Apkarian
Department of Chemistry, University of California, Irvine, California 92717

(Received 16 May 1995; accepted 27 June 1995)

Classical molecular dynamics simulations of quantum crystals, using a simple pseudopotential, are reported. The method is implemented for calculating both equilibrium and dynamical properties. As a test, the radial distribution functions for pure solid H_2 and Li doped solid H_2 are computed, and found to be in excellent agreement with prior results obtained by the variational Einstein model [D. Li and G. A. Voth, J. Chem. Phys. **96**, 5340 (1992)]. The method also yields a realistic phonon density of states, which is obtained by normal mode analysis. As an implementation in dynamics, the rotational motions of O_2 isolated in solid D_2 are investigated. In agreement with recent experiments, it is found that O_2 does not rotate in solid D_2. © *1995 American Institute of Physics.*

I. INTRODUCTION

Cryogenic crystals are among the simplest of systems in which details of many-body photodynamics can be investigated by iterating between experiment and simulation. While classical simulations of many particles are straightforward, dynamical treatments of many quantum degrees of freedom pose serious difficulties. At cryogenic temperatures, zero-point effects pose such a problem. To delineate the importance of such effects on dynamics we suffice by citing two examples. It has recently been demonstrated that femtosecond time resolved studies represent a uniquely powerful tool for the study of dynamics in cryogenic solids.[1] The information content in such measurements is directly related to the extent of classical coherence in the evolving dynamics. The extent of coherence has been demonstrated to be determined by the initial coordinate space distribution; which in turn, is controlled by zero-point amplitudes of lattice vibrations.[1] In another example, in statistical treatments of photodissociation quantum yields, it has been shown that dissociation probabilities near the energetic threshold are strictly determined by zero-point amplitudes of lattice vibrations, an effect that could not be treated by classical simulations alone.[2] Approximate methods, tailored to particular applications exist.[3–6] In the case of the time resolved studies,[1] temperature scaling was used as a method to account for the quantum amplitudes.[6] The systems mentioned above pertain to classical van der Waals solids, in which the quantum effects come into prominence due to the low working temperatures. Clearly the considerations are more severe in quantum hosts. We have in mind the significant body of recent work on spectroscopic studies of impurities isolated in condensed He,[7] and H_2.[8] Quite clearly, strictly classical simulations of dynamics in such media completely fail, and as we show below, temperature scaling yields completely unrealistic results. Convenient methods for incorporating quantum effects in dynamical simulations in an approximate, nevertheless, useful manner remain desirable.

The most common approach for simulating quantum many-body systems involves the path integral formulation of quantum statistical mechanics.[9] There is a vast literature on realizations of this principle in treatments of quantum hosts: solids, fluids, and clusters, which we do not cite here. We note, though, that these methods are inherently equilibrium calculations. In this report we test the utility of a conceptually simple dynamical approach, namely, classical dynamics simulations in which the single particles are represented by spatial Gaussian distributions. To test the method, we carry out simulations of solid *para*-hydrogen, both pure, and doped with Li. The latter system has recently been scrutinized by path integral Monte Carlo (PIMC) and a variational quantum Einstein model, with which we compare our results.[10,11] Having tested the reliability of the approach in obtaining equilibrium properties, we implement it in dynamical calculations, specifically considering the rotational dynamics of O_2 isolated in solid D_2, a system which was recently scrutinized by experiments.[12]

II. METHOD

Conceptually, the approach taken here is quite simple. We represent each particle by a Gaussian, and then classically simulate the time evolution of the centers of the Gaussians subject to the assumption of pairwise additivity of forces. The equations of motion for the centers of the Gaussians are then given according to Ehrenfest's theorem:

$$m\frac{d^2}{dt^2}\bar{r}_i \equiv m\frac{d^2}{dt^2}\langle r_i\rangle = \sum_{j\neq i}\langle -\nabla V(r_i-r_j)\rangle. \tag{1}$$

For isotropic pair potentials, functions of internuclear separation $R=|r_i-r_j|$ alone, the average force implied in Eq. (1) can be obtained for a pair of Gaussian particles by the convolution integral

$$\begin{aligned}\left\langle \frac{-\partial V_{ij}(\bar{R})}{\partial R}\right\rangle &\equiv \left\langle -\frac{\partial V(\bar{r}_i-\bar{r}_j)}{\partial(\bar{r}_i-\bar{r}_j)}\right\rangle \\ &= -\int_{-\infty}^{\infty} dr_i \int_{-\infty}^{\infty} dr_j G(r_i-\bar{r}_i) \\ &\quad \times G(r_j-\bar{r}_j)\frac{\partial V(r_i-r_j)}{\partial(r_i-r_j)} \\ &= -\int_{-\infty}^{\infty} dR G_{ij}(R-\bar{R})\frac{\partial V_{ij}(R)}{\partial R},\end{aligned} \tag{2a}$$

where

$$G_{ij}(R-\bar{R})=\frac{1}{2\sigma\sqrt{\pi}}\exp\left[-\frac{(R-\bar{R})^2}{4\sigma^2}\right]. \tag{2b}$$

While the definition of the average force is sufficient for numerical integration of Newton's equations of motion, it is generally more appealing to define a pseudopotential, $\tilde{V}_{ij}$, from which the pseudoforce can be obtained. This can be done by taking advantage of the local nature of the Gaussian function, and properties of the convolution integral

$$\begin{aligned}\left\langle -\frac{\partial V_{ij}(\bar{R})}{\partial R}\right\rangle &= -\int_{-\infty}^{\infty} dR G_{ij}(R-\bar{R})\frac{\partial V_{ij}(R)}{\partial R}\\ &= \int_{-\infty}^{\infty} dR V_{ij}(R)\frac{\partial G_{ij}(R-\bar{R})}{\partial R}\\ &= -\frac{\partial}{\partial R}\int_{\infty}^{\infty} dR V_{ij}(R) G_{ij}(R-\bar{R})\end{aligned} \tag{3}$$

$$\left\langle -\frac{\partial V_{ij}(\bar{R})}{\partial R}\right\rangle = -\frac{\partial}{\partial R}\langle V_{ij}(\bar{R})\rangle \equiv -\frac{\partial \tilde{V}_{ij}(\bar{R})}{\partial R}.$$

In practice $\tilde{V}_{ij}(\bar{R})$ is constructed by convolution of the pair potential, $V_{ij}(R)$, with a Gaussian, $G_{ij}(R)$, which represents the self-consistent pair probability distribution in the extended solid. Noting that at $T=0$ the pseudopotential represents the total zero-point energy, sum of potential and kinetic terms, a self-consistent criterion for the choice of the Gaussian width can be defined. Namely, it is demanded that minimization of the lattice sum of the pseudopotential

$$\frac{d\tilde{U}_{\text{tot}}}{dR}=\frac{d}{dR}\frac{1}{2}\sum_{ij}\tilde{V}(\bar{R}_{ij})=0 \tag{4}$$

yield the proper experimental lattice constant at $T=0$. For $\tilde{V}_{ij}(R)$ given as a function of powers of internuclear separation, the lattice sum can be evaluated and minimized analytically. For an arbitrary form, the width of the Gaussian can be chosen iteratively by numerically evaluating the lattice sum over the equilibrium configuration of the lattice. Given $\tilde{V}_{ij}$, classical molecular dynamics simulations can be carried out according to well-established prescriptions.[13] It is however important to note that the simulations are for the centers of the single particle distributions. While most observables can be computed directly, in the case of distributions, the output of the simulation has to be convoluted by the Gaussian once again. Thus, in the case of the radial distribution function, the simulation yields $g(\bar{R})$, and the proper distribution function, $g(R)$, is obtained as

$$g(R)=\int_{-\infty}^{\infty} d\bar{R} G(R-\bar{R}) g(\bar{R}). \tag{5}$$

A. Solid H_2

For simulations of solid H_2, we use the Silvera–Goldman pair potentials as $V_{ij}(R)$.[14] Note, this is an effective pair potential, implicitly incorporating many-body contributions. Using a Gaussian of width $\sigma=0.30$ Å in Eq. (2b), the constructed pseudopotential reproduces the lattice constant of solid H_2 ($a=3.79$ Å), which is nearly constant between $T=0$ and 4 K (at $T=4.2$ K, $P=0$, $V=23.16$ cc/mol).[15] The pair potential, the pseudopotential, and the Gaussian used are illustrated in Fig. 1. In the bound region, to within 0.1 K, $\tilde{V}_{ij}(\bar{R})$ can be fitted to the functional form (energies in eV and distances in Å)

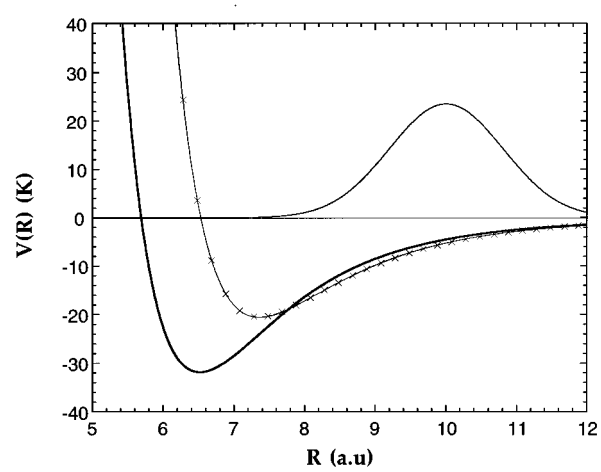

FIG. 1. The Silvera–Goldman pair potential for H_2 is shown (thick line) along with the pseudopotential (thin line) generated by convolution of the Gaussian, $G_{ij}(R)$, which is also shown. The hatch marks are from the analytic fit to the pseudopotential, Eq. (6) of text, which reproduces the numerical potential to within 0.1 K throughout the range shown.

$$\tilde{V}_{H_2-H_2}(\bar{R})=-\frac{26982}{\bar{R}^{12}}+\frac{9545.8}{\bar{R}^{10}}-\frac{630.24}{\bar{R}^{8}}+\frac{1.6385}{\bar{R}^{6}}, \tag{6}$$

which is a convenient form to be used in the numerical simulations (also illustrated in Fig. 1).

Classical molecular dynamics simulations were carried out in the microcanonical ensemble. A total of 640 p-H_2 molecules arranged on a hcp lattice were included in the simulation box, periodic boundary conditions, and the Verlet algorithm were implemented.[13] The H_2–H_2 radial distribution function, constructed according to Eq. (5), is shown in Fig. 2. Comparison of the radial distribution function with those of Li and Voth shows that the present result is indistinguishable from their converged variational Einstein model,[11] however, both are more structured than the fully converged PIMC simulations. The latter can be regarded as nearly exact.[10,11] Quite clearly, by freezing the zero-point energy in the pseudopotential the interparticle correlations are not well reproduced. It is interesting to note that if we do away with the criterion for the choice of the Gaussian width, then the PIMC results can be emulated. If we choose a Gaussian width nearly half that obtained by the energy minimization of Eq. (4), effectively unfreezing part of the zero-point energy, it is possible to approach the PIMC results. This is illustrated in Fig. 2 for a Gaussian width of 0.13 Å. However, given the arbitrary nature of this adjustment, we do not further pursue the procedure.

It is important to note that unlike a true Einstein model, the present pseudopotential produces a proper phonon spectrum. The phonon density of states for this system is determined by normal mode analysis, by diagonalizing the force

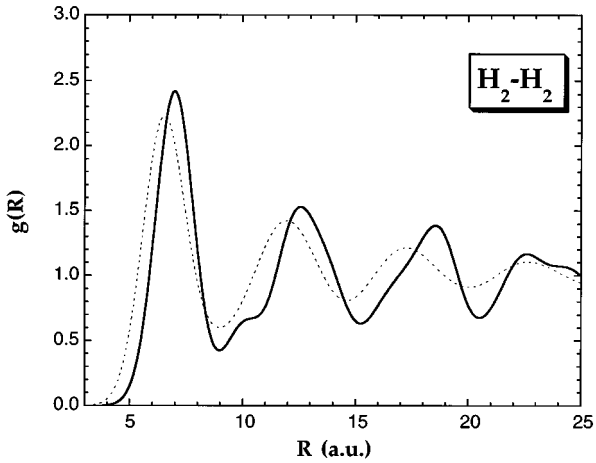

FIG. 2. Radial distribution function for solid H_2. Results of classical simulations using two different pseudopotentials are shown: solid line, is for the self-consistent pseudopotential generated by convolution of a Gaussian width $\sigma = 0.30$ Å [Eq. 2(b) of text]; dashed line, is for a pseudopotential generated by a Gaussian width of $\sigma = 0.13$ Å, while using the equilibrium lattice constant of the solid.

constant matrix. The results of diagonalization of the matrix for a cell containing 500 atoms (1500×1500 elements) is shown in Fig. 3. The density of states qualitatively agrees with that of solid H_2.[15,16] However, the computed frequencies are ~10% higher than that of solid H_2. As in the case of the structured distribution function, the implication is that the pseudopotential created based on the spatial Gaussian distribution yields too stiff a lattice. This result can also be amended by the use of a narrower Gaussian width.

B. Li doped H_2

We next consider solid H_2 doped with a single Li impurity atom. In contrast with the neat solid, in this case, a self-consistency criterion does not exist for the choice of a

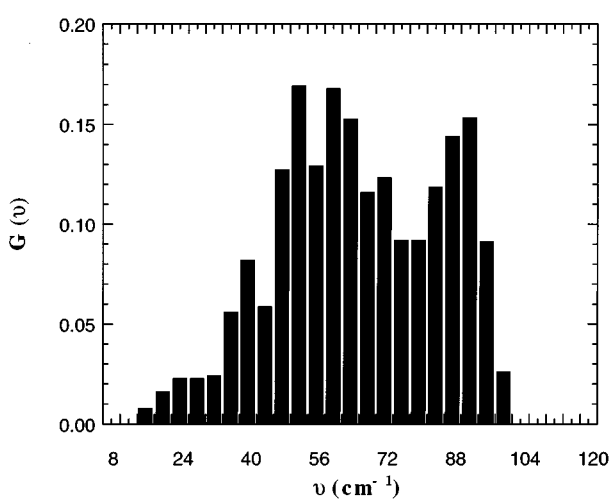

FIG. 3. Normal mode distribution of solid H_2 using the pseudopotential of Eq. (6) in text. The distribution is obtained by diagonalizing the force matrix for a lattice containing 500 H_2 molecules.

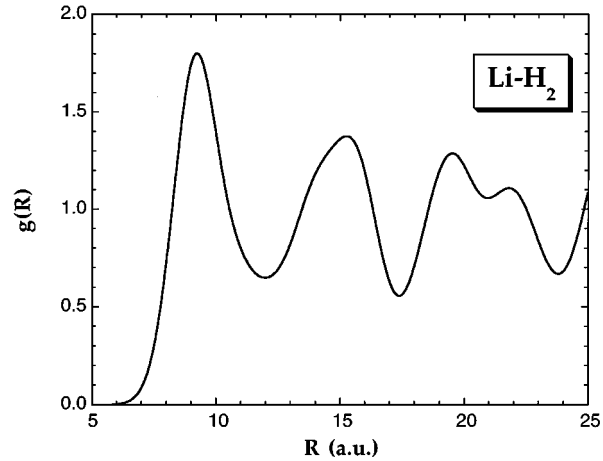

FIG. 4. Li–H_2 radial distribution function with Li occupying a fivefold substitutional site in hcp H_2.

Gaussian to generate the Li–H_2 pseudopotential. Given the fact that the Li–H_2 pair potential is extremely shallow, we do not expect localization of the H_2 function near the impurity. Moreover, since the solid is expected to anneal around the impurity for low doping densities, we expect that H_2 molecules nearest neighbor to Li will be well represented by their bulk single particle distributions. Accordingly, we construct the Li–H_2 pseudopotential using the same pair potential given in Ref. 11, and the Gaussian determined above for the neat solid. The resulting pseudopotential can be well fitted by a Morse function

$$\tilde{V}_{\mathrm{Li-H_2}}(\bar{R}) = D_e\{1-\exp[-\beta(\bar{R}-\bar{R}_e)]\}^2, \tag{7}$$

where $D_e = 1.05\times10^{-3}$ eV; $\bar{R}_e = 5.70$ Å, $\beta = 0.915$ Å^{-1}.

The classical simulations in this case are carried out by placing the Li atom in a cavity formed by removal of five nearest-neighbor atoms, which is one of the various trapping sites simulated in Ref. 11. The computed Li–H_2 pair distribution function is shown in Fig. 4. As in the case of pure H_2, the present result is indistinguishable from the converged variational Einstein model, and more structured than the converged PIMC results.[10(a)]

The above comparisons of equilibrium properties, the radial distribution functions, and the phonon spectrum, establish some confidence of the reliability of the method as a qualitative tool. Notwithstanding the simplicity of this approach, its major attraction is that it is inherently a dynamical treatment. We take advantage of this aspect in the example below.

C. Rotational dynamics of O_2 isolated in solid D_2

In recent experiments the spectroscopy of O_2 isolated in solid D_2 was investigated.[12] Based on a detailed analysis of the spectra, including polarized laser-induced fluorescence measurements, it was established that O_2 molecules isolated in fcc sites of the solid do not rotate. In principle such an issue can be trivially resolved by simulations in classical solids. However, in the case of quantum crystals, strictly classical simulations completely fail. With periodic bound-

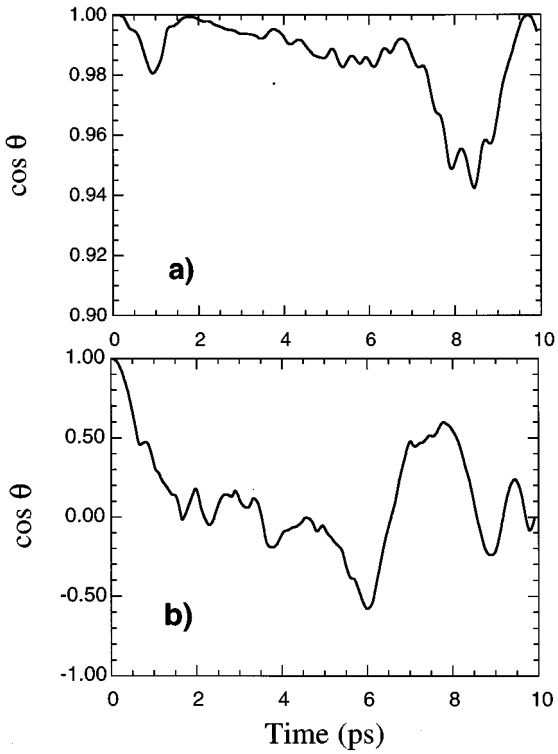

FIG. 5. Rotational dynamics of O_2 isolated in solid D_2. The time evolution of the O_2 axis is shown as a function of time; (a) using pseudopotentials defined in Eq. (9) of text, (b) using pair potentials and a scaled temperature of $T'=50$ K$\sim\theta_D/2$. Note the change in ordinate scales between the two plots.

aries it is possible to carry out classical simulations without having the crystal collapse. However, if the experimental temperatures, 3–5 K, are used in the simulations, then all motion is frozen in a metastable ground state. The metastability of the solid is due to the well-known fact that in the absence of zero-point energy the pair potentials produce imaginary phonon frequencies.[14] In fact, small perturbations of the simulation box lead to lattice melting and diffusion of atoms. The temperature scaling method employed in simulations of classical solids also fail. In this case, the recipe calls for simulations at an effective temperature T', which produces the proper amplitude of single particle motion, where T' is related to the real temperature T through[1,6,17]

$$T'=\frac{\hbar\omega}{2k_B}\left(\tanh\left(\frac{\hbar\omega}{2k_BT}\right)\right)^{-1}\approx\frac{\hbar\omega}{2k_B}, \tag{8}$$

where $\hbar\omega/k_B=124$ K, is the Debye frequency of the solid.[15] Accordingly, the scaled particle kinetic energies exceed the pair binding energy, and therefore the simulation corresponds in effect to that of a lattice gas. Again, the energetics is highly unstable, and now nearly free rotation of the molecule is observed. We illustrate in Figs. 5(a) and 5(b), the results of simulations by the pseudopotential and the scaled temperature methods, respectively. The time evolution of the projection of the molecular axis, $\cos\theta=\hat{\mathbf{R}}(t)\cdot\hat{\mathbf{R}}(0)$, is shown. In the case of classical simulations with $T'\sim50$ K, complete rotation is possible [Fig. 5(b)]. When the pseudopotential approach is used, the lattice is stable, and the molecular rotation is completely frozen [see Fig. 5(a)], in agreement with the experiment.

The pair potentials used in these simulations are given below. The O–D_2 potential was assumed to be that of O–Ne, which has been obtained from scattering data.[18] The pseudopotentials were generated as in the case of Li/H_2, by using the self-consistent Gaussian width which reproduces the lattice constant for neat *ortho*-D_2. The D_2–D_2 and O–D_2 pseudopotentials (energies in eV and distances in Å) are

$$\tilde{V}_{D_2-D_2}(\bar{R})=-\frac{23571}{\bar{R}^{12}}+\frac{7413.1}{\bar{R}^{10}}-\frac{488.13}{\bar{R}^{8}}-\frac{0.21182}{\bar{R}^{6}}, \tag{9a}$$

$$\tilde{V}_{O-D_2}(\bar{R})=\frac{15181}{\bar{R}^{12}}-\frac{1315.5}{\bar{R}^{10}}+\frac{55.516}{\bar{R}^{8}}-\frac{10.729}{\bar{R}^{6}}. \tag{9b}$$

III. CONCLUSIONS

We have described an approach for molecular dynamics simulations of quantum crystals, which despite its simplicity, seems to produce quite realistic results. The method, relies on the assumption of a Gaussian spatial probability distribution for single particles, based on which a pseudopotential is generated without any adjustable parameters. Strictly classical dynamics is then simulated using these pseudopotentials, which represents a standard computational task. The radial distribution functions calculated via strictly classical simulations on these pseudopotentials then yield results that are nearly identical to those of Li and Voth, obtained by the vibrational Einstein model method.[11] Moreover, a realistic phonon spectrum is obtained. However, in contrast with Monte Carlo methods, the approach can be implemented in dynamical applications. The latter was demonstrated in calculations of rotational motions of O_2 in solid D_2.

In its present formulation, the method described only produces a qualitative picture. The radial distribution functions for example do not match exactly with those of the converged path integral Monte Carlo calculations.[10] This disagreement was shown to be due to the complete freezing of zero-point kinetic energy in the pseudopotential. This suggests obvious refinements to the treatment. In particular, the use of thawed Gaussian wave packets in the simulations could be expected to produce improved results with some increase in computational effort.[19] Such an implementation is being presently pursued by us.

ACKNOWLEDGMENTS

This research was supported under grants from the US Air Force Office of Scientific Research: Nos. AFOSRF 49620-1-0251 and F49620-95-1-0213. Helpful discussions with C. C. Martens are gratefully acknowledged.

[1] R. Zadoyan, Z. Li, C. C. Martens, and V. A. Apkarian, J. Chem. Phys. **101**, 6648 (1994).
[2] J. Zoval and V. A. Apkarian, J. Phys. Chem. **98**, 7945 (1994).

[3] P. Jungworth and R. B. Gerber, J. Chem. Phys. **102**, 6046 (1995).
[4] N. Makri, Chem. Phys. Lett. **193**, 435 (1992).
[5] G. Voth, D. Chandler, and W. H. Miller, J. Chem. Phys. **91**, 7749 (1989).
[6] J. P. Bergsma, P. H. Berens, K. R. Wilson, D. F. Fredkin, and E. Heller, J. Phys. Chem. **88**, 612 (1984).
[7] B. Tabbert, M. R. Beau, J. Fischer, and G. Z. Putlitz, Phys. B **194**, 731 (1994); Y. Takahashi, K. Sano, T. Kinoshita, and T. Yabuzaki, Phys. Rev. Lett. **71**, 1035 (1993); M. Arndt, S. I. Kanorsky, A. Weis, and T. W. Hansch, *ibid*. **74**, 1359 (1995).
[8] M. E. Fajardo, S. Tam, T. L. Thompson, and M. E. Cordonnier, Chem. Phys. **189**, 351 (1994), and references therein.
[9] R. P. Feynman and A. R. Hibbs, *Quantum Mechanics and Path Integrals* (McGraw-Hill, New York, 1965).
[10] (a) D. Scharf, G. J. Martyna, D. Li, G. A. Voth, and M. Klein, J. Chem. Phys. **99**, 9013 (1993); (b) D. Scharf, G. J. Martyna, and M. Klein, *ibid*. **99**, 8997 (1993).
[11] D. Li and G. A. Voth, J. Chem. Phys. **96**, 5340 (1992).
[12] A. Danilychev, V. E. Bondybey, V. A. Apkarian, S. Tanaka, H. Kajihara, and S. Koda, J. Chem. Phys. (in press).
[13] M. P. Allen and D. J. Tildesley, *Computer Simulations of Liquids* (Clarendon, Oxford, 1987).
[14] I. F. Silvera and V. V. Goldman, J. Chem. Phys. **69**, 4209 (1978).
[15] I. F. Silvera, Rev. Mod. Phys. **52**, 393 (1980).
[16] V. V. Goldman, J. Low Temp. Phys. **36**, 521 (1979).
[17] J. P. Bergsma, P. H. Berens, K. R. Wilson, D. F. Fredkin, and E. Heller, J. Phys. Chem. **88**, 612 (1984).
[18] V. Aquilanti, R. Candori, and F. Pirani, J. Chem. Phys. **89**, 6157 (1988).
[19] E. J. Heller, J. Chem. Phys. **62**, 1544 (1975).